

Flavoured Neutrinoless Double Beta Decay

Lukas Graf,^{1,*} Sudip Jana,^{1,†} Manfred Lindner,^{1,‡} Werner Rodejohann,^{1,§} and Xun-Jie Xu^{1,2,¶}

¹Max-Planck-Institut für Kernphysik, Saupfercheckweg 1, 69117 Heidelberg, Germany

²Service de Physique Théorique, Université Libre de Bruxelles,
Boulevard du Triomphe, CP225, 1050 Brussels, Belgium

We discuss a mechanism of neutrinoless double beta decay, where neutrinos of different flavours come into play. This is realized by effective flavour-violating scalar interactions. As one consequence, we find that within the normal mass ordering the neutrino effective mass may no longer vanish due to contributions from other flavours. We evaluate the necessary nuclear matrix elements, consider the interference between the standard diagram and the new scalar one, and analyze a UV-complete model that realizes the scalar interaction. Tests of the complete model are possible at colliders and future neutrino experiments. Our scenario represents an alternative mechanism for neutrinoless double beta decay, where nevertheless lepton number violation resides only in Majorana mass terms of light neutrinos.

I. INTRODUCTION

Neutrinoless double beta ($0\nu\beta\beta$) decay [1], referring to the conversion of a nucleus

$$(A, Z) \rightarrow (A, Z + 2) + 2e^-, \quad (1)$$

is of great interest to particle physics and cosmology [2–4]. Its observation would imply the non-conservation of lepton number, a charge associated with an accidental global Abelian symmetry of the Standard Model (SM). It would also mean that a Majorana neutrino mass is generated at certain (possibly tiny) level, hence, neutrinos can be identified with their own antiparticles [5, 6]. Given its importance, an extensive worldwide experimental effort is being made to observe $0\nu\beta\beta$ decay [7, 8]. The current best experimental lower limits on $0\nu\beta\beta$ decay half-life are already above 10^{26} y [9, 10].

In the standard interpretation of the decay, see Fig. 1, internally at each W -electron vertex an electron neutrino appears, and the necessary spin flip renders the amplitude proportional to the *effective mass* $U_{ei}^2 m_i \equiv m_{ee}$. Here $U_{\alpha i}$ are elements of the leptonic mixing matrix and m_i the neutrino masses; this combination is furthermore nothing but the ee -element of the neutrino mass matrix. Since the W boson mass is much larger than the nuclear scale, the standard diagram can be described by two effective left-handed $u_L d_L e_L (\nu_e)_L$ vertices with a long-range Majorana neutrino exchange leading to a m_{ee} mass-insertion, see Fig. 1. The parameters allow for a complete cancellation in case of a normal hierarchy, $m_{ee} = 0$, which would lead to infinitely long lifetimes. This corresponds to the “funnel” appearing in the usual plot of the effective mass in dependence on the lightest neutrino mass, see Fig. 3.

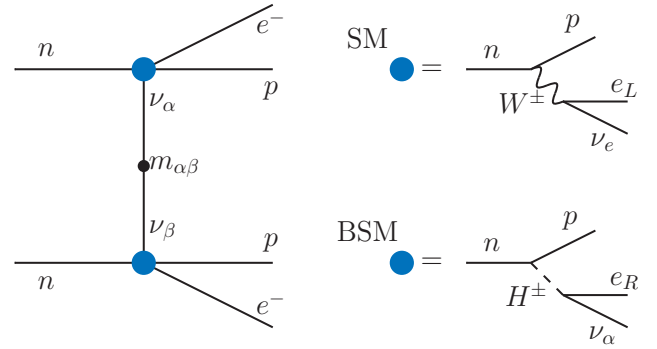


Figure 1. Flavoured double beta decay in and beyond the Standard Model. The standard diagram with mass-insertion m_{ee} contains two SM-vertices generated by a W -exchange. A new flavour-violating vertex generated by a charged scalar particle allows for a mass-insertion $m_{\alpha\beta}$.

As commonly known, there exist several possibilities to generate the $0\nu\beta\beta$ decay with new physics [2, 3]. We propose here the “flavoured” version of the decay. That is, a mechanism with one or both of the left-handed $u_L d_L e_L (\nu_e)_L$ vertices replaced by a beyond-the-Standard-Model scalar one, $u_L d_R e_R (\nu_\alpha)_L$ (see Fig. 1). In this case, a $m_{\alpha\beta} = U_{\alpha i} U_{\beta i} m_i$ mass-insertion can arise. This $u_L d_R e_R (\nu_\alpha)_L$ flavour-violating, but lepton number conserving, vertex could originate from integrating out a charged scalar particle. The corresponding mass matrix elements $m_{\alpha\beta}$ have a different behavior as a function of the smallest neutrino mass and the mass ordering than m_{ee} (see Fig. B1), hence the usual interpretation and phenomenology of the decay is altered. Our scenario is distinctive from other alternative $0\nu\beta\beta$ mechanisms, as the new contribution to neutrinoless double beta decay depends on neutrino parameters. That is, lepton number violation occurs only in the Majorana mass terms of the light neutrinos.

Since the new contribution is suppressed by a mass-insertion and the constraint on the new scalar effective interaction, one may believe that its contribution is hope-

* E-mail: lukas.graf@mpi-hd.mpg.de

† E-mail: sudip.jana@mpi-hd.mpg.de

‡ E-mail: manfred.lindner@mpi-hd.mpg.de

§ E-mail: werner.rodejohann@mpi-hd.mpg.de

¶ E-mail: xunjie.xu@mpi-hd.mpg.de

less to observe. However, the nuclear matrix elements of the new contribution are enhanced, owing to a pion-exchange contribution, which somewhat compensates the double suppression.

Indeed, we demonstrate in this paper that using this effective framework current limits from neutrino oscillation and other experiments allow for in principle observable half-lives of $0\nu\beta\beta$ decay mediated by the flavoured diagram, with numbers corresponding to half-lives implied by meV-scale effective masses. Moreover, the different dependence on the neutrino parameters contained in $m_{\alpha\beta}$ means that the usual phenomenology of the decay is altered. For instance, within the normal mass ordering the lifetime may no longer be infinitely long due to parameter cancellations, i.e. the “funnel” gets sealed.

We then investigate options to generate the scalar $u_L d_R e_R(\nu_\alpha)_L$ vertex with new physics in UV-complete models, focusing on a weak singlet charged scalar related to neutrino mass generation. This brings along additional experimental constraints, for instance from oscillation data or colliders.

II. FLAVOURED $0\nu\beta\beta$ DECAY RATE

Let us consider the following interactions

$$\mathcal{L}_{\text{int}} = \mathcal{L}_V + \mathcal{L}_S, \quad (2)$$

$$\mathcal{L}_V = 2\sqrt{2}G_F V_{ud} [\bar{u}\gamma^\mu P_L d] [\bar{e}\gamma_\mu P_L \nu_e] + \text{h.c.}, \quad (3)$$

$$\mathcal{L}_S = 2\sqrt{2}G_F \epsilon_\alpha V_{ud} [\bar{u}P_L d] [\bar{e}P_L \nu_\alpha] + \text{h.c.} \quad (4)$$

Here \mathcal{L}_V is the SM charged current (CC) interaction responsible for $0\nu\beta\beta$, and \mathcal{L}_S contains a new 4-fermion non-standard interaction (NSI) of the scalar form, sometimes also referred to as a generalized neutrino interaction (GNI) [11]. Further, G_F is the Fermi constant, V is the CKM matrix, $P_L = (1 - \gamma^5)/2$ is the left-handed projector, and ϵ_α is a flavour-dependent coupling characterizing the strength of the new interaction. The projector in the quark sector in Eq. (4) could be also right-handed, but it would not affect the result significantly. We stress here that the operator in Eq. (4) conserves lepton number. Therefore, lepton number violation is only triggered by the Majorana mass terms of the light neutrinos. This implies that our new contribution to neutrinoless double beta decay will depend on neutrino parameters, which distinguishes it from most other alternative mechanisms.

Given the above Lagrangian (2), $0\nu\beta\beta$ decay is in principle generated by the standard diagram with two left-handed vector vertices (depending on m_{ee}), a diagram with one left-handed vector vertex replaced by the scalar one (depending on $m_{e\alpha}$), and a diagram with both vertices being of a scalar nature (depending on $m_{\alpha\beta}$). It turns out, however, that the mechanism combining the SM and BSM vertices vanishes at the leading order in our approximation; hence, we neglect it and focus only on the two other contributions. These are related to different nuclear matrix elements (NMEs), which we denote

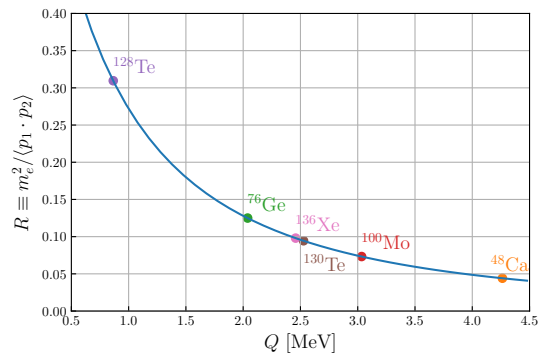


Figure 2. The interference factor R is defined in Eq. (8) as a function of the Q value.

within this work as vector (M_V) and scalar (M_S). The two diagrams will interfere with each other, with the size of the interference term depending on the chirality of the electrons. The energies of the emitted electrons are larger than their mass by a factor of a few, which sets the order of magnitude of the interference term on the amplitude level.

Combining both the standard and the new physics contributions, the decay rate is given by (for details of the derivation, see Appendix A)

$$\Gamma_{0\nu} = \frac{G_{0\nu}}{m_e^2} |\tilde{m}_{ee} M_V|^2, \quad (5)$$

where $G_{0\nu}$ is the phase space factor, M_V is the nuclear matrix element of the standard $0\nu\beta\beta$ process, m_e is the electron mass, and \tilde{m}_{ee} is defined to include both the standard (m_{ee}) and flavoured ($m_{\alpha\beta}$) contributions as

$$\tilde{m}_{ee} \equiv |m_{ee}|^2 + |S|^2 + 2 \text{Re}[R S m_{ee}^*]. \quad (6)$$

Here we have defined combined quantity of particle and nuclear physics parameters,

$$S \equiv m_{\alpha\beta} \epsilon_\alpha \epsilon_\beta \frac{M_S}{M_V}, \quad (7)$$

and the interference factor of the diagrams

$$R \equiv \frac{\int_p m_e^2}{\int_p E_1 E_2}. \quad (8)$$

The notation \int_p stands for a phase space integral,

$$\int_p F \equiv \int F \delta(\Delta M - E_1 - E_2) \frac{|\mathbf{p}_1|^2 |\mathbf{p}_2|^2 d|\mathbf{p}_1| d|\mathbf{p}_2|}{(2\pi)^4 E_1 E_2}, \quad (9)$$

where we denote the two out-going electron momenta by \mathbf{p}_1 and \mathbf{p}_2 , their energies by $E_{1,2} = \sqrt{|\mathbf{p}_{1,2}|^2 + m_e^2}$ and the mass difference between the initial and final nuclei by ΔM , which is connected to the Q value as $\Delta M =$

NME	M_V	M_S
^{76}Ge	-6.46	131
^{136}Xe	-3.57	70.5

Table I. Numerical values of the nuclear matrix elements obtained using the IBM-2 nuclear structure framework [12–14] for the standard and the flavoured $0\nu\beta\beta$ decay mechanisms. Note the large numbers for the NME M_S corresponding to the mechanism involving two copies of the scalar interaction, which are a consequence of the enhancement by the pionic resonance involved.

$Q + 2m_e$. In Fig. 2 we show R for a variety of relevant isotopes.

Considering the NMEs, as mentioned in the introduction, the scalar ones enjoy an enhancement due to the pionic resonance manifesting through a large pseudoscalar nucleon form factor, which can be understood given the structure of these NMEs discussed in detail in Appendix A 2. The numerical values of the total NMEs obtained for ^{76}Ge and ^{136}Xe using the Interacting Boson Model (IBM-2) [12–14] are summarized in Table I.

For an explicit example we need the experimental limits on the scalar coupling ϵ_α . At first, note that in neutrino oscillation experiments, this scalar interaction does not influence neutrino propagation but can cause flavour transition at zero distance. In addition, CKM unitarity and leptonic universality also provide strong bounds. According to Refs. [15, 16], the strongest bounds for e and τ flavours come from CKM unitarity, and for the μ flavour from neutrino oscillation experiments. Also note that in Refs. [15, 16], only bounds on vector interactions (i.e., $\epsilon_\alpha^V [\bar{u}\gamma^\mu P_L d] [\bar{e}\gamma_\mu P_L \nu_\alpha]$) were provided. Properly translated in our ϵ_α (overall rates differ by a factor 2 due to the different Lorentz structure), the bounds are $\epsilon_\mu < 0.052$ and $\epsilon_\tau < 0.082$ at 90% CL. There is also a more updated analysis on the bound from beta decay [17] (the bound from CKM unitarity in Ref. [15] is based on beta decay combined with meson decay data), which reads $\epsilon < 0.063$ at 90% CL for right-handed neutrinos with scalar interactions. Since for the case of muon and tau neutrinos interference with the SM processes is absent, this bound can be directly interpreted as a bound on ϵ_μ and ϵ_τ . Combining the bounds in the literature, we conclude that the current bounds on ϵ_μ and ϵ_τ are

$$\epsilon_\mu < 0.052, \quad \epsilon_\tau < 0.063 \quad (90\% \text{ CL}). \quad (10)$$

As for ϵ_e , due to interference in beta decay, the bound is much more stringent and it is also more complicated to convert the beta decay bounds on the vector ϵ_e^V to the scalar one because in this case the chirality flipping of e_L/e_R is involved. Here we simply ignore the possibility of non-zero ϵ_e , which would simply be a minor rescaling of the $0\nu\beta\beta$ decay half-life.

For non-zero ϵ_μ and ϵ_τ , $0\nu\beta\beta$ decay depends on $m_{\mu\mu}$

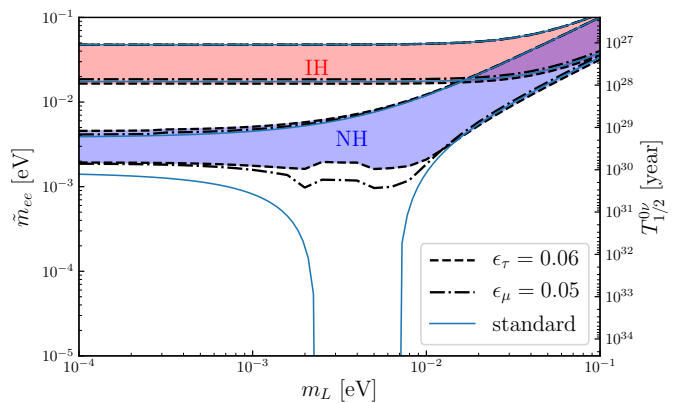


Figure 3. The effect of scalar interactions on $0\nu\beta\beta$. Here, m_L is the lightest neutrino mass and \tilde{m}_{ee} is defined in Eq. (6). The solid curves represent the standard $0\nu\beta\beta$ without new interactions; the other curves include the new physics contributions ($\epsilon_\tau = 0.06$ (dashed) and $\epsilon_\mu = 0.05$ (dash-dotted)). We took here the isotope ^{76}Ge , the interference factor of which is $R = 0.12$.

and $m_{\tau\tau}$, respectively. In case of ϵ_μ and ϵ_τ both being non-zero, $m_{\mu\tau}$ contributes in addition to \tilde{m}_{ee} . Of course, the standard diagram depending on m_{ee} is also present. Using the values in Eq. (10), we show in Fig. 3 the (modified) effective mass as a function of the smallest neutrino mass m_L . We stress again the funnel for $m_L \in [0.002, 0.007]$ eV, where m_{ee} vanishes due to cancellations. However, for our example, \tilde{m}_{ee} can not vanish anymore. This is due to the different behavior of $m_{\alpha\beta} \neq m_{ee}$ as a function of the smallest neutrino mass, cf. Fig. B1. The usual funnel is now sealed. Note that we also include the corresponding half-life of the decay in the plot. The numbers are large, as they correspond to meV-scale effective masses. The NMEs that we have calculated (for details see Appendix A) use the IBM-2 approach. Those matrix elements are known to lead to larger half-lives than some of the other approaches such as those based on the Energy Density Functional (see [18] for a comparison), so that one could easily obtain smaller values. There are however also approaches which would lead to larger half-lives, such as the Shell Model. This is of course the usual dilemma in calculations of NMEs. Note further that we choose a quenched value of $g_A = 1$ for the axial coupling.

We stress here the importance of the scalar nature of the new interaction. Its effect is the reduction of the interference term, which means that a complete cancellation of the standard and new physics diagram is not possible.

III. UV COMPLETION

Let us now analyze an explicit realization of the effective scalar interaction. As a prototypical example, we consider the Zee model [19] – one of the most popular

neutrino mass models, where neutrino masses and mixings are generated via quantum corrections at one-loop level, while NSIs are induced at tree level via exchange of charged scalar particles. The particle content of the Zee model contains an $SU(2)_L$ -doublet scalar H_2 and $SU(2)_L$ -singlet charged scalar η^\pm , in addition to the SM-like Higgs doublet H_1 . Although the Wolfenstein version of the model [20] which assumes an additional Z_2 symmetry, is ruled out by oscillation data [21, 22], it has been recently shown that the original version of the model [19] is perfectly consistent with the neutrino oscillation data [23, 24].

Following similar conventions, we adopt the scalar potential and the resulting mass spectrum from Ref. [24]. The cubic coupling $(\mu H_1^i H_2^j \eta^- \epsilon_{ij} + \text{h.c.})$ in the scalar potential leads to mixing between η^+ and H_2^+ , with a mixing angle denoted as φ and the physical charged Higgs states denoted as h^+ and H^+ , respectively. Here, we work in a rotated basis for the Higgs doublets [25] in which only the neutral Higgs H_1 has a nonzero vacuum expectation value v . Now, one can express the Yukawa Lagrangian as

$$\begin{aligned} \mathcal{L}_y = & Y_d \bar{Q}_L d_R H_1 + \tilde{Y}_d \bar{Q}_L d_R H_2 + Y_u \bar{Q}_L u_R \tilde{H}_1 \\ & + \tilde{Y}_u \bar{Q}_L u_R \tilde{H}_2 + Y_\ell \bar{\psi}_L H_1 \psi_R + \tilde{Y}_\ell \bar{\psi}_L H_2 \psi_R \quad (11) \\ & + f \bar{\psi}^c_L \psi_L \eta^+ + \text{h.c.}, \end{aligned}$$

where the left-handed lepton and quark doublets are denoted as $\psi_L = (\nu, e)_L^T$ and $Q_L = (u, d)_L^T$. Neutrino masses and mixings are generated radiatively at one-loop level as [19] $M_\nu = \kappa(f M_\ell Y_\ell + \tilde{Y}_\ell^T M_\ell f^T)$, with the charged lepton mass matrix $M_\ell = Y_\ell v / \sqrt{2}$ and $16\pi^2 \kappa = \sin 2\varphi \log(m_{h^+}^2 / m_{H^+}^2)$. As we can see, the product of the Yukawa couplings f and \tilde{Y}_ℓ is constrained from neutrino oscillation data. In what follows, we will denote the entries of Y_ℓ and \tilde{Y}_ℓ as $Y_{\alpha\beta}$ and $\tilde{Y}_{\alpha\beta}$, respectively. In order to maximize the scalar interaction in the model [24], we adopt the choice $\tilde{Y}_\ell = \mathcal{O}(1)$ and $f \ll 1$ here. Since both Higgs doublets couple to up and down type quarks, a coupling between the charged Higgs h^+ (which is mostly the singlet) and up-down type quarks will be induced via the \tilde{Y}_q term due to mixing with the charged Higgs H^+ (mostly the doublet). Indeed, due to the presence of both couplings \tilde{Y}_ℓ and \tilde{Y}_q , the scalar coupling ϵ_α is generated by

$$\epsilon_\alpha = \frac{1}{4\sqrt{2}G_F} \left(\frac{|\tilde{Y}_{\alpha e} \tilde{Y}_{ud}| \sin^2 \varphi}{m_{h^+}^2} + \frac{|\tilde{Y}_{\alpha e} \tilde{Y}_{ud}| \cos^2 \varphi}{m_{H^+}^2} \right). \quad (12)$$

Moreover, the leptonic Yukawa \tilde{Y}_ℓ itself leads to an effective four-fermion Lagrangian relevant for vector NSI in the form

$$\mathcal{L}_{\text{eff}} = (\bar{\nu}_\tau e_R) (\bar{e}_R \nu_\tau) \left(\frac{|\tilde{Y}_{\tau e}|^2 \sin^2 \varphi}{m_{h^+}^2} + \frac{|\tilde{Y}_{\tau e}|^2 \cos^2 \varphi}{m_{H^+}^2} \right),$$

where we consider the τ flavour of neutrino ($\tilde{Y}_{\tau e} \neq 0$) for simplicity and to avoid other stringent limits from lepton

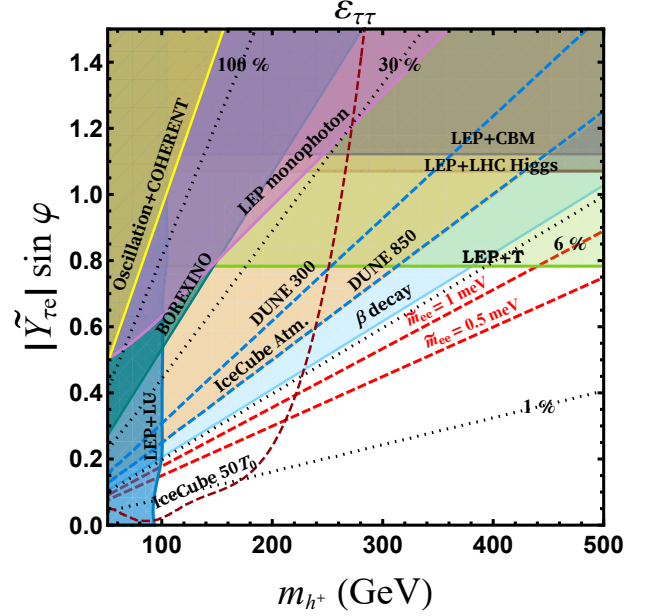


Figure 4. Implications of the charged Higgs in the Zee model. The red dashed lines are derived assuming non-observation of $0\nu\beta\beta$ in future experiments sensitive to $\tilde{m}_{ee} = 1$ meV and 0.5 meV. Different color shaded regions are excluded from different experiments, black dotted lines depict the Zee model predictions for diagonal leptonic NSI $\epsilon_{\tau\tau}$ and the other color dashed lines indicate the future sensitivity of different upcoming experiments; see text for details.

universality tests in W decays [26] and Michel parameter constraints [27]. Applying the Fierz transformation, we can rewrite it as

$$\mathcal{L}_{\text{eff}} = -\frac{1}{2} (\bar{\nu}_\tau \gamma_\mu \nu_\tau) (\bar{e}_R \gamma^\mu e_R) \left(\frac{|\tilde{Y}_{\tau e}|^2 \sin^2 \varphi}{m_{h^+}^2} + \frac{|\tilde{Y}_{\tau e}|^2 \cos^2 \varphi}{m_{H^+}^2} \right),$$

which can be directly compared to the standard parametrization of NSI in the form [28]

$$\mathcal{L}_{\text{NSI}}^{\text{NC}} = -2\sqrt{2}G_F \sum_{f, X, \alpha, \beta} \epsilon_{\alpha\beta}^{fX} (\bar{\nu}_\alpha \gamma^\mu P_L \nu_\beta) (\bar{f} \gamma_\mu P_X f).$$

Hence, at the tree level, the leptonic NSI induced by the singly-charged scalars h^\pm, H^\pm is given by

$$\epsilon_{\tau\tau}^{eR} \equiv \epsilon_{\tau\tau} = \frac{1}{4\sqrt{2}G_F} \left(\frac{|\tilde{Y}_{\tau e}|^2 \sin^2 \varphi}{m_{h^+}^2} + \frac{|\tilde{Y}_{\tau e}|^2 \cos^2 \varphi}{m_{H^+}^2} \right). \quad (13)$$

In the quark sector, even if one starts with a diagonal texture of Yukawa matrices \tilde{Y}_q , off-diagonal entries reappear due to non-vanishing CKM entries. This is why we assume all the scalars originating primarily from the second doublet reside above the TeV scale and that all entries except the (1,1) one in both the up-type and down-type quark Yukawa matrices are sufficiently small in order to avoid flavor-changing neutral current (FCNC) processes.

However, there will be still strong constraints from meson decays, CKM unitarity, the T parameter, beta decay, etc. As mentioned earlier, the most stringent bound originates from beta decay combined with meson decay data, which reads $\epsilon_\tau < 0.063$. In the lepton sector, there will be stringent constraints from charged lepton flavour violating processes. However, we make such judiciary choice in Yukawa matrices \tilde{Y}_ℓ ($\tilde{Y}_{\tau e} \neq 0, Y_{\alpha\tau} \neq 0$ for $\alpha = e$ or μ) that no more than one entry in a given row of \tilde{Y}_ℓ is large. Such a choice (keeping only the entries ($\tilde{Y}_{ee}, \tilde{Y}_{\mu e}, \tilde{Y}_{\tau e}$) one at a time in the first column of \tilde{Y}_ℓ) does not lead to $\ell_\alpha \rightarrow \ell_\beta + \gamma$ decay mediated by the charged scalar and also does not affect the maximum strength of the NSI. These choices also automatically satisfy LEP contact interaction limits for the process $e^-e^+ \rightarrow f\bar{f}$ [24]. With this choice, the charged scalar, h^+ , can be as light as ~ 110 GeV, while satisfying all these experimental constraints [24]. The LHC contact interaction limits are also not directly applicable if the charged scalar h^+ is that light. Further note that, our choice of parameter space leads to the dominant decay mode of $h^+ \rightarrow \tau\nu$, and thus, it can escape the stringent LHC constraint imposed by analyses looking for charged lepton (e or μ) and missing transverse momentum events. In a Nevertheless, there will be still several theoretical and experimental constraints, such as charge breaking minima, electroweak precision tests, charged lepton flavour violation, collider constraints from LEP and LHC, lepton universality tests and monophoton constraints, all of which are shown in Fig. 4. The yellow, dark-green and orange shaded regions depict the direct constraints on $\epsilon_{\tau\tau}$ from a global fit to neutrino oscillation + COHERENT data [29], neutrino-electron scattering experiments such as Borexino [30], and IceCube atmospheric neutrino data [31], respectively. The purple shaded region is excluded by the monophoton process $e^+e^- \rightarrow \nu\bar{\nu}\gamma$ from LEP data [32], since the $e\nu\nu$ operator leads to an additional contribution for the process mediated by h^+ in the t -channel. In order to maximize leptonic NSI, a large mixing between the singlet and doublet charged scalar fields, and hence, a large trilinear μ term needs to be introduced. However, it cannot be arbitrarily large, since it leads to charge breaking minima of the potential. This limit is shown by the gray shaded region. A light charged scalar additionally contributes to the $h \rightarrow \gamma\gamma$ process and the limit from LHC Higgs data [33] is shown as the brown shaded region. The light green colored region is excluded by the T parameter [27]. LEP

constraints on charged scalar searches are shown by the blue shaded region. The blue dashed lines indicate the future DUNE sensitivities on $\epsilon_{\tau\tau}$ for 300 and 850 kt MW yr exposure [34]. At IceCube, the light charged scalar h^+ of the model could potentially lead to a Glashow-like resonance feature [35] in the ultra-high energy neutrino event spectrum; the dashed brown curve indicates this future IceCube sensitivity corresponding to an exposure time of $50 \times T_0$ [35], where $T_0 = 2653$ days. For completeness of our study, we set $\tilde{Y}_{\tau e} = \tilde{Y}_{ud}$ in Fig. 4 to find a direct correlation between ϵ_τ and $\epsilon_{\tau\tau}$. The cyan region is excluded from the β decay limit. The red dashed lines are derived assuming non-observation of $0\nu\beta\beta$ decay in future experiments sensitive to \tilde{m}_{ee} of 1 meV and 0.5 meV.

IV. CONCLUSION

We have pointed out that neutrinoless double beta decay can be mediated by a general $m_{\alpha\beta}$ mass-insertion, instead of the usually considered standard mechanism with its m_{ee} mass-insertion. This can be realized via new lepton number conserving scalar interactions.

The funnel of neutrinoless double beta decay of infinite half-life can be sealed in this way, which we demonstrated explicitly. A UV completion of the new scalar interaction within the Zee model of radiative neutrino mass generation was shown to be in agreement with all existing limits from neutrino oscillations to collider physics.

While the absence of the funnel can be expected in any scenario with more than one contribution to $0\nu\beta\beta$ decay, the new mechanism discussed here depends on the lightest neutrino mass. Lepton number violation is only implied by the Majorana mass term of the light neutrinos.

Appendix A: Derivation of the $0\nu\beta\beta$ Decay Half-Life

1. Particle Physics

In the presence of the new interactions in Eq. (4), the amplitude of $0\nu\beta\beta$ decay is modified to

$$i\mathcal{M}_{V+S}^{(0\nu\beta\beta)} = \langle e_1 e_2 F | (\mathcal{L}_V + \mathcal{L}_S) (\mathcal{L}_V + \mathcal{L}_S) | I \rangle, \quad (\text{A1})$$

where $\langle F |$ and $| I \rangle$ are the final and initial nuclear states, and $\langle e_1 e_2 |$ denotes the final electron states. Expanding Eq. (A1), we obtain

$$i\mathcal{M}_{V+S}^{(0\nu\beta\beta)} = (8G_F^2 V_{ud}^2) \int \frac{d^4q}{(2\pi)^4} \left\{ [i\mathcal{M}_S^{(\text{lep})}] [i\mathcal{M}_S^{(\text{nuc})}] + [i\mathcal{M}_{SV}^{(\text{lep})}]^\mu [i\mathcal{M}_{SV}^{(\text{nuc})}]_\mu + [i\mathcal{M}_V^{(\text{lep})}]^{\mu\nu} [i\mathcal{M}_V^{(\text{nuc})}]_{\mu\nu} \right\}, \quad (\text{A2})$$

where $\mathcal{M}_X^{(\text{lep})}$ and $\mathcal{M}_X^{(\text{nuc})}$ are the leptonic and nuclear parts of the amplitude, and q is the internal momentum. The subscripts S, V , and SV of the partial amplitudes indicate that they are from $\mathcal{L}_S\mathcal{L}_S, \mathcal{L}_V\mathcal{L}_V$, and $\mathcal{L}_V\mathcal{L}_S$ or $\mathcal{L}_S\mathcal{L}_V$ in Eq. (A1).

The leptonic amplitudes read

$$i\mathcal{M}_S^{(\text{lep})} = \bar{u}_e P_L \frac{i}{\not{q}} (-i\epsilon_\alpha m_{\alpha\beta} \epsilon_\beta) \frac{i}{\not{q}} P_L u_{e^c} = \bar{u}_e \frac{im_{\alpha\beta} \epsilon_\alpha \epsilon_\beta}{q^2} P_L u_{e^c}, \quad (\text{A3})$$

$$i\mathcal{M}_{SV}^{(\text{lep})} = \bar{u}_e \gamma^\mu P_L \frac{i}{\not{q}} (-im_{e\beta} \epsilon_\beta) \frac{i}{\not{q}} P_L u_{e^c} + \bar{u}_e P_L \frac{i}{\not{q}} (-i\epsilon_\alpha m_{\alpha e}) \frac{i}{\not{q}} P_L \gamma^\mu u_{e^c} = \bar{u}_e \frac{im_{e\beta} \epsilon_\beta}{q^2} \gamma^\mu u_{e^c}, \quad (\text{A4})$$

$$i\mathcal{M}_V^{(\text{lep})} = \bar{u}_e \gamma^\mu P_L \frac{i}{\not{q}} (-im_{ee}) \frac{i}{\not{q}} P_L \gamma^\nu u_{e^c} = \bar{u}_e \frac{im_{ee}}{q^2} \gamma^\mu \gamma^\nu P_R u_{e^c}, \quad (\text{A5})$$

where q is the neutrino momentum, \bar{u}_e and u_{e^c} are the two electron final states, and $m_{\alpha\beta}$ is an element of the neutrino mass matrix. After antisymmetrizing the above three expressions in the electron wave functions (i.e. taking both t and u diagrams into account), the second one, combining the SM vector and BSM scalar vertices, vanishes. The corresponding contribution could be in principle still saved by a compensating minus sign coming from the nuclear part of the amplitude. However, this would require inclusion of electron P wave, and thus would result in a subleading contribution, which we neglect. We explicitly checked this does not affect our conclusions.

The relevant nuclear amplitudes, defined as

$$i\mathcal{M}_S^{(\text{nuc})} \equiv \langle F | \bar{u} P_L d \bar{u} P_L d | I \rangle, \quad (\text{A6})$$

$$i\mathcal{M}_V^{(\text{nuc})} \equiv \langle F | \bar{u} \gamma^\mu P_L d \bar{u} \gamma^\nu P_L d | I \rangle, \quad (\text{A7})$$

give rise, after applying the hadronization procedure (described e.g. in Ref. [36]), to the nuclear matrix elements M_S and M_V corresponding to the purely scalar and the standard vector contribution, respectively. The structure of these is discussed in more detail in the next subsection.

Combining the leptonic and nuclear amplitudes, we obtain

$$i\mathcal{M}_{V+S}^{(0\nu\beta\beta)} = i\bar{u}_e [\lambda_V P_R + \lambda_S P_L] u_{e^c}, \quad (\text{A8})$$

where

$$(\lambda_V, \lambda_S) \propto (m_{ee} M_V, m_{\alpha\beta} \epsilon_\alpha \epsilon_\beta M_S). \quad (\text{A9})$$

Applying the trace technology, we obtain the following squared amplitude

$$\begin{aligned} \left| i\mathcal{M}_{V+S}^{(0\nu\beta\beta)} \right|^2 &= \text{Tr} \{ u_e \bar{u}_e [\lambda_V P_R + \lambda_S P_L] u_{e^c} \bar{u}_{e^c} [\lambda_V^* P_L + \lambda_S^* P_R] \} \\ &= 2p_1 \cdot p_2 [|\lambda_V|^2 + |\lambda_S|^2] + 2m_e^2 [\lambda_S \lambda_V^* + \lambda_V \lambda_S^*]. \end{aligned} \quad (\text{A10})$$

Here, we are considering $S_{1/2}$ approximation of the electron wave functions. We have used $u_e \bar{u}_e = \not{p}_1 + m_e$ and $u_{e^c} \bar{u}_{e^c} = \not{p}_2 + m_e$, with p_1 and p_2 being the two momenta of the outgoing electrons.

The decay rate of $0\nu\beta\beta$ is computed by (see the appendix of Ref. [37])

$$\Gamma_{0\nu} = \int \frac{\left| i\mathcal{M}_{V+S}^{(0\nu\beta\beta)} \right|^2 2\pi\delta}{4M_N(M_N - \Delta M)} \left[\prod_{i=1}^2 \frac{d^3 p_i}{(2\pi)^3 2E_i} \right], \quad (\text{A11})$$

where M_N is the mass of the initial nucleus, ΔM is the mass difference between the final and the initial nuclei, and

$$\delta = \delta(\Delta M - E_1 - E_2). \quad (\text{A12})$$

Note that in the above phase space integral, the spatial part of $p_1 \cdot p_2$ in $\left| i\mathcal{M}_{V+S}^{(0\nu\beta\beta)} \right|^2$ does not contribute because

$$\int p_1 \cdot p_2 \prod_{i=1}^2 \frac{d^3 p_i}{(2\pi)^3 2E_i} \delta \int (E_1 E_2 - |\mathbf{p}_1| |\mathbf{p}_2| \cos \theta) \frac{|\mathbf{p}_1|^2 |\mathbf{p}_2|^2 d|\mathbf{p}_1| d|\mathbf{p}_2| d\cos \theta}{(2\pi)^4 2E_1 E_2} \delta = \int E_1 E_2 \frac{|\mathbf{p}_1|^2 |\mathbf{p}_2|^2 d|\mathbf{p}_1| d|\mathbf{p}_2|}{(2\pi)^4 E_1 E_2} \delta,$$

where θ is the angle between \mathbf{p}_1 and \mathbf{p}_2 . The spatial part vanishes when θ is integrated out.

Now we define

$$R \equiv \frac{\int_p m_e^2}{\int_p E_1 E_2}, \quad (\text{A13})$$

with the notation $\int_p F \equiv \int F \frac{|\mathbf{p}_1|^2 |\mathbf{p}_2|^2 d|\mathbf{p}_1| d|\mathbf{p}_2|}{(2\pi)^4 E_1 E_2} \delta$ for an arbitrary function F . Then, in order to compute Eq. (A11), one simply needs to replace $p_1 \cdot p_2 \rightarrow \int_p E_1 E_2$, $E_1 E_2 \rightarrow \int_p E_1 E_2$, $m_e^2 \rightarrow \int_p m_e^2$ in Eq. (A10).

Therefore, our final result of $0\nu\beta\beta$ decay rate including the new interaction reads

$$\Gamma_{0\nu} = \frac{G_{0\nu}}{m_e^2} \left[|m_{ee} M_V|^2 + |m_{\alpha\beta} \epsilon_\alpha \epsilon_\beta M_S|^2 \right] + \frac{G_{0\nu}}{m_e^2} 2R \text{Re} [m_{\alpha\beta} \epsilon_\alpha \epsilon_\beta M_S m_{ee}^* M_V^*]. \quad (\text{A14})$$

Here R , defined in Eq. (A13), is referred to as *interference factor*. Given an isotope dependent Q , with $\Delta M = Q + 2m_e$, R can be evaluated numerically according to Eq. (A13). In Fig. 2, we present the $R(Q)$ curve and indicate the values for several typical isotopes.

2. Nuclear Matrix Elements

For the derivation of the relevant nuclear matrix elements (NMEs) entering the rate of the studied $0\nu\beta\beta$ decay contributions we follow the standard procedure described in detail e.g. in Ref. [36]. Hence, after parametrizing the nucleon matrix elements of the considered quark bilinears in terms of the nucleon form factors $F_X(q)$ we make use of the nonrelativistic expansion and obtain an approximate expression for individual currents, combinations of which give the actual NMEs. As usual, we consider only $0^+ \rightarrow 0^+$ transition.

For the standard mechanism we use the usual expression (see e.g. [38], where the same notation was used) giving the total NME M_V as

$$M_V = g_V^2 M_F - g_A^2 M_{GT}^{AA} + \frac{g_{A9P}}{6} (M_{GT}^{AP} + M_T^{AP}) + \frac{(g_V + g_W)^2}{12} (-2M_{GT}^{WW} + M_T^{WW}) - \frac{g_P^2}{48} (M_{GT}^{PP} + M_T^{PP}). \quad (\text{A15})$$

Here, the form factor charges g_X correspond to the value of the nucleon form factors $F_X(q)$ at zero momentum transfer, i.e. $g_X = F_X(0)$. We employ the following numerical values: $g_V = 1$, $g_A = 1$, $g_W = 3.7$, $g_P = 231$ [39], $g_S = 1$ [17], $g_{P'} = 349$ [17]. We assume a quenching of the effective nuclear axial coupling, as often employed in the literature, see e.g. the discussion in Ref. [38]. The large values of the pseudoscalar couplings g_P and $g_{P'}$ are due to enhancement by the implicit pion resonance. The dependence on the momentum q transferred between the two beta-decaying nucleons captured by the product of the reduced form factors $F_X(q^2)/g_X$ is then incorporated within the elementary nuclear matrix elements entering Eq. (A15). Table II shows the explicit form of the individual Fermi (M_F), Gamow-Teller (M_{GT}) and tensor (M_T) NMEs including the corresponding reduced form factor products $\tilde{h}(q^2)$.

All the NMEs defined in Tab. II contain on top of the product of the reduced nucleon form factors $\tilde{h}(q^2)$ also the neutrino potential, which captures the q dependence of the long-range exchange of an essentially massless neutrino mediating the $0\nu\beta\beta$ decay. As we follow the formulation of [39] and [13], the two-body transition operator is constructed in momentum space. The neutrino potential for the studied mechanisms reads

$$v(q) = \frac{2}{\pi} \frac{1}{q(q + \tilde{A})}. \quad (\text{A16})$$

Here, given the typical neutrino momentum q , the neutrino mass has been neglected and \tilde{A} denotes the closure energy, taken from Ref. [41] or estimated by the systematics, and finally $\tilde{A} = 1.12A^{1/2}$ MeV.

In the same spirit we derive the NMEs contributing to the scalar $0\nu\beta\beta$ decay mechanism discussed here. The product of two scalar nucleon currents can be expressed as

$$M_S = g_S^2 M_F + \frac{g_{P'}^2}{12} (M_{GT}^{P'P'} - M_T^{P'P'}), \quad (\text{A17})$$

where the elementary NMEs on the right-hand side are defined in Tab. II.

To calculate the numerical values of the derived NMEs a nuclear structure model must be employed. Here, we make use of so called Interacting Boson Model (IBM-2) [12–14].

<i>Standard Mechanism</i>	
NME	$\tilde{h}_o(q^2)$
$M_F = \langle h_{XX}(q^2) \rangle$	$\tilde{h}_{XX}(q^2) = \frac{1}{(1+q^2/m_V^2)^4}$
$M_{GT}^{WW} = \left\langle \frac{\mathbf{q}^2}{m_p^2} h_{XX}(q^2) (\boldsymbol{\sigma}_a \cdot \boldsymbol{\sigma}_b) \right\rangle$	$\tilde{h}_{XX}(q^2)$
$M_T^{WW} = \left\langle \frac{\mathbf{q}^2}{m_p^2} h_{XX}(q^2) \mathbf{S}_{ab} \right\rangle$	$\tilde{h}_{XX}(q^2)$
$M_{GT}^{AA} = \langle h_{AA}(q^2) (\boldsymbol{\sigma}_a \cdot \boldsymbol{\sigma}_b) \rangle$	$\tilde{h}_{AA}(q^2) = \frac{1}{(1+q^2/m_A^2)^4}$
$M_{GT}^{AP} = \left\langle \frac{\mathbf{q}^2}{m_p^2} h_{AP}(q^2) (\boldsymbol{\sigma}_a \cdot \boldsymbol{\sigma}_b) \right\rangle$	$\tilde{h}_{AP}(q^2) = \frac{1}{(1+q^2/m_A^2)^4} \frac{1}{1+q^2/m_\pi^2}$
$M_T^{AP} = \left\langle \frac{\mathbf{q}^2}{m_p^2} h_{AP}(q^2) \mathbf{S}_{ab} \right\rangle$	$\tilde{h}_{AP}(q^2)$
$M_{GT}^{PP} = \left\langle \frac{\mathbf{q}^4}{m_p^4} h_{PP}(q^2) (\boldsymbol{\sigma}_a \cdot \boldsymbol{\sigma}_b) \right\rangle$	$\tilde{h}_{PP}(q^2) = \frac{1}{(1+q^2/m_A^2)^4} \frac{1}{(1+q^2/m_\pi^2)^2}$
$M_T^{PP} = \left\langle \frac{\mathbf{q}^4}{m_p^4} h_{PP}(q^2) \mathbf{S}_{ab} \right\rangle$	$\tilde{h}_{PP}(q^2)$
<i>Flavoured Scalar Mechanisms</i>	
NME	$\tilde{h}_o(q^2)$
$M_{GT}^{P'P'} = \left\langle \frac{\mathbf{q}^2}{m_p^2} h_{PP}(q^2) (\boldsymbol{\sigma}_a \cdot \boldsymbol{\sigma}_b) \right\rangle$	$\tilde{h}_{PP}(q^2)$
$M_T^{P'P'} = \left\langle \frac{\mathbf{q}^2}{m_p^2} h_{PP}(q^2) \mathbf{S}_{ab} \right\rangle$	$\tilde{h}_{PP}(q^2)$

Table II. Here we list the double beta decay Fermi (M_F), Gamow-Teller (M_{GT}) and tensor (M_T) NMEs entering Eqs. (A15) and (A17). The relevant reduced form factor product $\tilde{h}(q^2)$ is always shown alongside. These q -dependent functions enter the NMEs multiplied by the neutrino potential given in Eq. (A16); hence we define, $h_o(q^2) = v(q^2)\tilde{h}_o(q^2)$. The label X in the above definitions stands collectively for vector, weak-magnetism and tensor form factors involved, i.e. $X = V, W, T$, as all of these come with the same shape parameter $m_V = 0.84$ GeV [40]. The q dependencies of the axial and pseudoscalar form factors denoted by subscripts A and P , respectively, include the shape parameter $m_A = 1.09$ GeV [40] and for the pion mass we take $m_\pi = 0.138$ GeV. The spin operators corresponding to individual nucleons a, b are represented using the Pauli matrices $\boldsymbol{\sigma}_{a,b}$ and the tensor NMEs incorporate the operator $S_{ab} = 3(\boldsymbol{\sigma}_a \cdot \mathbf{q})(\boldsymbol{\sigma}_b \cdot \mathbf{q}) - (\boldsymbol{\sigma}_a \cdot \boldsymbol{\sigma}_b)$.

Appendix B: Magnitudes of neutrino mass matrix elements

In addition to m_{ee} , neutrino mass matrix elements of other flavours are also involved in this work. It is therefore useful to know their magnitudes and dependence on the smallest mass m_L , which have been studied in the literature – see [42, 43]. For the reader's convenience (and also as an update), in this appendix we display in Fig. B1 the magnitudes of all neutrino mass matrix elements.

ACKNOWLEDGMENTS

The authors would like to thank Frank F. Deppisch and Oliver Scholer for useful comments. LG is grateful to Jose Barea for providing the code to calculate the standard mechanism of double beta decay in the IBM-2 framework.

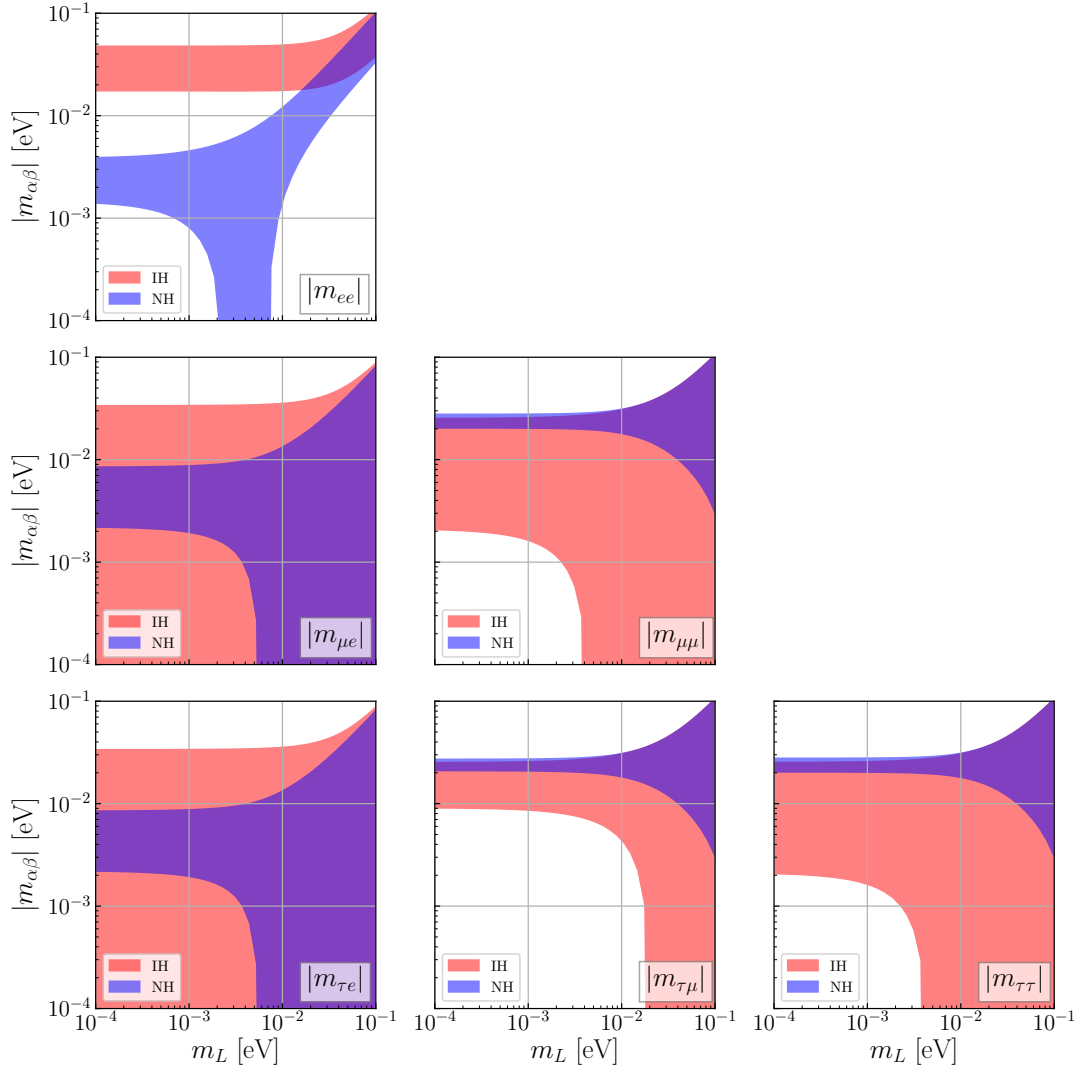


Figure B1. The individual neutrino mass matrix elements against the smallest neutrino mass m_L , see also [42, 43]. Note the funnel appearing in the m_{ee} case.

- [1] W. Furry, “On transition probabilities in double beta-disintegration,” *Phys. Rev.* **56** (1939) 1184–1193.
- [2] W. Rodejohann, “Neutrino-less Double Beta Decay and Particle Physics,” *Int. J. Mod. Phys. E* **20** (2011) 1833–1930, [arXiv:1106.1334 \[hep-ph\]](#).
- [3] F. F. Deppisch, M. Hirsch, and H. Päs, “Neutrinoless Double Beta Decay and Physics Beyond the Standard Model,” *J. Phys. G* **39** (2012) 124007, [arXiv:1208.0727 \[hep-ph\]](#).
- [4] F. F. Deppisch, L. Graf, J. Harz, and W.-C. Huang, “Neutrinoless Double Beta Decay and the Baryon Asymmetry of the Universe,” *Phys. Rev. D* **98** no. 5, (2018) 055029, [arXiv:1711.10432 \[hep-ph\]](#).
- [5] J. Schechter and J. Valle, “Neutrinoless Double beta Decay in SU(2) x U(1) Theories,” *Phys. Rev. D* **25** (1982) 2951.
- [6] M. Duerr, M. Lindner, and A. Merle, “On the Quantitative Impact of the Schechter-Valle Theorem,” *JHEP* **06** (2011) 091, [arXiv:1105.0901 \[hep-ph\]](#).
- [7] S. Dell’Oro, S. Marcocci, M. Viel, and F. Vissani, “Neutrinoless double beta decay: 2015 review,” *Adv. High Energy Phys.* **2016** (2016) 2162659, [arXiv:1601.07512 \[hep-ph\]](#).
- [8] M. J. Dolinski, A. W. Poon, and W. Rodejohann, “Neutrinoless Double-Beta Decay: Status and Prospects,” *Ann. Rev. Nucl. Part. Sci.* **69** (2019) 219–251, [arXiv:1902.04097 \[nucl-ex\]](#).
- [9] **KamLAND-Zen** Collaboration, A. Gando *et al.*, “Search for Majorana Neutrinos near the Inverted Mass Hierarchy Region with KamLAND-Zen,” *Phys. Rev. Lett.* **117** no. 8, (2016) 082503, [arXiv:1605.02889 \[hep-ex\]](#). [Addendum: *Phys.Rev.Lett.* 117, 109903 (2016)].
- [10] **GERDA** Collaboration, M. Agostini *et al.*, “Final Results of GERDA on the Search for Neutrinoless Double- β Decay,” [arXiv:2009.06079 \[nucl-ex\]](#).
- [11] I. Bischer and W. Rodejohann, “General neutrino interactions from an effective field theory perspective,” *Nucl. Phys. B* **947** (2019) 114746, [arXiv:1905.08699 \[hep-ph\]](#).
- [12] J. Barea and F. Iachello, “Neutrinoless double-beta decay in the microscopic interacting boson model,” *Phys. Rev. C* **79** (2009) 044301.
- [13] J. Barea, J. Kotila, and F. Iachello, “Nuclear matrix elements for double- β decay,” *Phys. Rev. C* **87** no. 1, (2013) 014315, [arXiv:1301.4203 \[nucl-th\]](#).
- [14] J. Barea, J. Kotila, and F. Iachello, “ $0\nu\beta\beta$ and $2\nu\beta\beta$ nuclear matrix elements in the interacting boson model with isospin restoration,” *Phys. Rev. C* **91** no. 3, (2015) 034304, [arXiv:1506.08530 \[nucl-th\]](#).
- [15] C. Biggio, M. Blennow, and E. Fernandez-Martinez, “General bounds on non-standard neutrino interactions,” *JHEP* **08** (2009) 090, [arXiv:0907.0097 \[hep-ph\]](#).
- [16] Y. Farzan and M. Tortola, “Neutrino oscillations and Non-Standard Interactions,” *Front.in Phys.* **6** (2018) 10, [arXiv:1710.09360 \[hep-ph\]](#).
- [17] M. González-Alonso, O. Naviliat-Cuncic, and N. Severijns, “New physics searches in nuclear and neutron β decay,” *Prog. Part. Nucl. Phys.* **104** (2019) 165–223, [arXiv:1803.08732 \[hep-ph\]](#).
- [18] J. Engel and J. Menéndez, “Status and Future of Nuclear Matrix Elements for Neutrinoless Double-Beta Decay: A Review,” *Rept. Prog. Phys.* **80** no. 4, (2017) 046301, [arXiv:1610.06548 \[nucl-th\]](#).
- [19] A. Zee, “A Theory of Lepton Number Violation, Neutrino Majorana Mass, and Oscillation,” *Phys. Lett.* **93B** (1980) 389. [Erratum: *Phys. Lett.* 95B,461(1980)].
- [20] L. Wolfenstein, “A Theoretical Pattern for Neutrino Oscillations,” *Nucl. Phys.* **B175** (1980) 93–96.
- [21] Y. Koide, “Can the Zee model explain the observed neutrino data?,” *Phys. Rev.* **D64** (2001) 077301, [arXiv:hep-ph/0104226 \[hep-ph\]](#).
- [22] X.-G. He, “Is the Zee model neutrino mass matrix ruled out?,” *Eur. Phys. J.* **C34** (2004) 371–376, [arXiv:hep-ph/0307172 \[hep-ph\]](#).
- [23] J. Herrero-Garcia, T. Ohlsson, S. Riad, and J. Wiren, “Full parameter scan of the Zee model: exploring Higgs lepton flavor violation,” *JHEP* **04** (2017) 130, [arXiv:1701.05345 \[hep-ph\]](#).
- [24] K. Babu, P. B. Dev, S. Jana, and A. Thapa, “Non-Standard Interactions in Radiative Neutrino Mass Models,” *JHEP* **03** (2020) 006, [arXiv:1907.09498 \[hep-ph\]](#).
- [25] K. S. Babu and S. Jana, “Enhanced Di-Higgs Production in the Two Higgs Doublet Model,” *JHEP* **02** (2019) 193, [arXiv:1812.11943 \[hep-ph\]](#).
- [26] **LEP, ALEPH, DELPHI, L3, OPAL, LEP Electroweak Working Group, SLD Electroweak Group, SLD Heavy Flavor Group** Collaboration, “A Combination of preliminary electroweak measurements and constraints on the standard model,” [arXiv:hep-ex/0312023 \[hep-ex\]](#).
- [27] **Particle Data Group** Collaboration, M. Tanabashi *et al.*, “Review of Particle Physics,” *Phys. Rev.* **D98** no. 3, (2018) 030001.
- [28] L. Wolfenstein, “Neutrino Oscillations in Matter,” *Phys. Rev.* **D17** (1978) 2369–2374.
- [29] I. Esteban, M. C. Gonzalez-Garcia, M. Maltoni, I. Martinez-Soler, and J. Salvado, “Updated Constraints on Non-Standard Interactions from Global Analysis of Oscillation Data,” *JHEP* **08** (2018) 180, [arXiv:1805.04530 \[hep-ph\]](#).
- [30] **Borexino** Collaboration, S. K. Agarwalla *et al.*, “Constraints on Non-Standard Neutrino Interactions from Borexino Phase-II,” [arXiv:1905.03512 \[hep-ph\]](#).
- [31] A. Esmaili and A. Yu. Smirnov, “Probing Non-Standard Interaction of Neutrinos with IceCube and DeepCore,” *JHEP* **06** (2013) 026, [arXiv:1304.1042 \[hep-ph\]](#).
- [32] Z. Berezhiani and A. Rossi, “Limits on the nonstandard interactions of neutrinos from e^+e^- colliders,” *Phys. Lett.* **B535** (2002) 207–218, [arXiv:hep-ph/0111137 \[hep-ph\]](#).
- [33] **ATLAS** Collaboration, “A combination of measurements of Higgs boson production and decay using up to 139 fb^{-1} of proton–proton collision data at $\sqrt{s} = 13\text{ TeV}$ collected with the ATLAS experiment,”.
- [34] P. S. B. Dev, “NSI and Neutrino Mass Models at DUNE,”. <https://indico.fnal.gov/event/18430/session/6/contribution/23/material/slides/0.pdf>.
- [35] K. Babu, P. Dev, S. Jana, and Y. Sui, “Zee-Burst: A New Probe of Neutrino Nonstandard Interactions at

- IceCube,” *Phys. Rev. Lett.* **124** no. 4, (2020) 041805, [arXiv:1908.02779 \[hep-ph\]](#).
- [36] L. Graf, F. F. Deppisch, F. Iachello, and J. Kotila, “Short-Range Neutrinoless Double Beta Decay Mechanisms,” *Phys. Rev. D* **98** no. 9, (2018) 095023, [arXiv:1806.06058 \[hep-ph\]](#).
- [37] F. F. Deppisch, L. Graf, W. Rodejohann, and X.-J. Xu, “Neutrino Self-Interactions and Double Beta Decay,” *Phys. Rev. D* **102** no. 5, (2020) 051701, [arXiv:2004.11919 \[hep-ph\]](#).
- [38] F. F. Deppisch, L. Graf, F. Iachello, and J. Kotila, “Analysis of Light Neutrino Exchange and Short-Range Mechanisms in $0\nu\beta\beta$ Decay,” [arXiv:2009.10119 \[hep-ph\]](#).
- [39] F. Simkovic, G. Pantis, J. Vergados, and A. Faessler, “Additional nucleon current contributions to neutrinoless double beta decay,” *Phys. Rev. C* **60** (1999) 055502, [arXiv:hep-ph/9905509](#).
- [40] M. Schindler and S. Scherer, “Nucleon Form Factors of the Isovector Axial-Vector Current: Situation of Experiments and Theory,” *Eur. Phys. J. A* **32** no. 4, (2007) 429–433, [arXiv:hep-ph/0608325](#).
- [41] W. Haxton and G. Stephenson, “Double beta Decay,” *Prog. Part. Nucl. Phys.* **12** (1984) 409–479.
- [42] A. Merle and W. Rodejohann, “The Elements of the neutrino mass matrix: Allowed ranges and implications of texture zeros,” *Phys. Rev. D* **73** (2006) 073012, [arXiv:hep-ph/0603111](#).
- [43] W. Grimus and P. Ludl, “Correlations of the elements of the neutrino mass matrix,” *JHEP* **12** (2012) 117, [arXiv:1209.2601 \[hep-ph\]](#).